Eur. J. Mineral., 37, 143–149, 2025
https://doi.org/10.5194/ejm-37-143-2025

European Journal of Mineralogy
Open Access

$Fe^{3+}/\Sigma Fe$ variation in lawsonite and epidote in subducted oceanic crust

Donna L. Whitney[1], **Max Wilke**[2], **Sara E. Hanel**[1], **Florian Heidelbach**[3], **Olivier Mathon**[4], and **Angelika D. Rosa**[4]

[1]Department of Earth and Environmental Sciences, University of Minnesota, Minneapolis, MN 55455, USA
[2]Institut für Geowissenschaften, Universität Potsdam, 14476 Potsdam-Golm, Germany
[3]Bayerisches Geoinstitut, Universität Bayreuth, 95440 Bayreuth, Germany
[4]European Synchrotron Radiation Facility, Grenoble, 38000, France

Correspondence: Donna L. Whitney (dwhitney@umn.edu)

Received: 4 September 2024 – Revised: 16 December 2024 – Accepted: 7 January 2025 – Published: 7 March 2025

Abstract. The hydrous Ca–Al silicates lawsonite and epidote group minerals (EGMs) are key phases in subduction-zone H_2O and element cycling. In high-pressure–low-temperature metamorphic rocks, Fe in both minerals is typically assumed to be entirely Fe^{3+}, which substitutes for Al in octahedral sites as a major component in most EGMs and as a minor component in lawsonite and zoisite. New Fe micro-X-ray absorption near-edge spectroscopy (μ-XANES) analyses show substantial Fe^{2+} in lawsonite in blueschist from New Caledonia and zoisite from an unknown locality. Analysed Fe-rich EGMs (epidote, clinozoisite) contain primarily Fe^{3+}. Lawsonite and some EGMs in subducted oceanic crust may contain more Fe^{2+} than is currently known, with possible implications for understanding subduction redox processes and conditions and why they vary in different subduction zones.

1 Introduction

Hydrous silicates such as lawsonite (~ 11.5 wt % H_2O) and epidote group minerals (~ 2 wt % H_2O) are significant in volatile and element cycling in subduction zones via (de)hydration reactions, with implications for the oxidation state of subducted materials and subsequently the overlying mantle and volcanic arcs (e.g. Schmidt and Poli, 1994; Spandler et al., 2003; Frei et al., 2004; Martin et al., 2011, 2014; Vitale Brovarone et al., 2014; Whitney et al., 2020; Muñoz-Montecinos et al., 2021; Kang et al., 2022; Hernández-Uribe and Tsujimori, 2023). The presence of these modally abundant minerals in metamorphosed oceanic crust also influences the geophysical properties and geodynamic behaviour of subducted slabs (e.g. Kita et al., 2006; Chantel et al., 2012; Shiraishi et al., 2022). Furthermore, they are important index minerals of subduction metamorphic conditions, with lawsonite indicating colder pressure–temperature (P–T) conditions and epidote group minerals indicating relatively warm conditions; e.g. at ~ 2 GPa, lawsonite is stable at $T <$ ca. 550 °C and zoisite/epidote is stable at $T >$ ca. 550 °C.

Iron is a major element in epidote and a more minor component in lawsonite and some epidote group minerals (EGMs) (e.g. near-end-member clinozoisite, zoisite). In high-pressure–low-temperature (HP/LT) metabasalts, Fe in lawsonite and EGMs is typically assumed to be Fe^{3+} that substitutes for Al^{3+} in octahedral sites because there is generally good correspondence of Fe vs. Al in epidote-(clino)zoisite with low rare-earth-element (REE) content (e.g. Fornash et al., 2019). Ferric iron only or dominant compositions ($Fe^{3+}/\Sigma Fe \sim 1$) have been confirmed by Mössbauer spectroscopy (Weber et al., 2007) and X-ray absorption near-edge spectroscopy (XANES) (this study) for some lawsonite as well as for some epidote (Mössbauer: Grodzicki et al., 2001; XANES: Wilke et al., 2001; this study). Thus far, Fe^{2+}-bearing lawsonite has only been reported for one of three samples of lawsonite from the Franciscan subduction complex analysed in a Mössbauer spectroscopy study (Weber et al., 2007); in that paper, Fe^{2+}-bearing lawsonite was

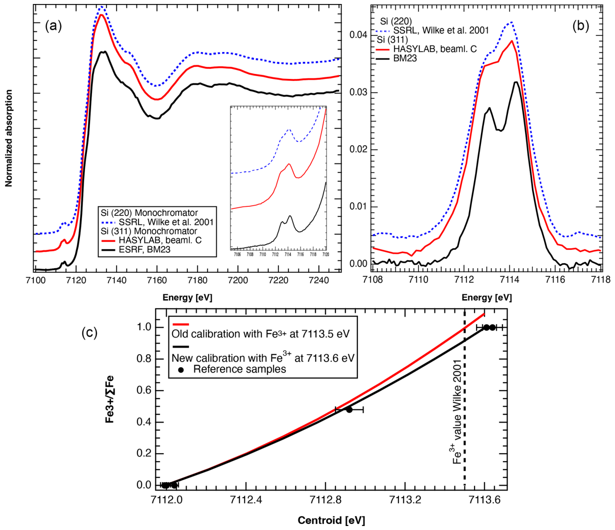

Figure 1. **(a)** Comparison of normalized XANES spectra of aegirine reference sample illustrating the spectral resolution measured at beamlines and with monochromators indicated. The inset shows a zoomed-in view of the pre-edge region. **(b)** Pre-edge after background subtraction. **(c)** Variation in the centroid with $Fe^{3+}/\Sigma Fe$. Comparison of old calibration (Wilke et al., 2009) and new calibration. Plotted reference samples include olivine, almandine garnet, omphacite, and aegirine. SSRL is the Stanford Synchrotron Radiation Lightsource.

determined to have a composition of $(Ca_{0.97}Fe^{2+}_{0.01})(Al_{0.98}, Fe^{3+}_{0.02})_2Si_2O_7(OH)_2 \cdot H_2O$. Here we report new Fe K-edge μ-XANES analyses documenting substantial amounts of Fe^{2+} and variation in $Fe^{3+}/\Sigma Fe$ in some lawsonite and EGMs in blueschist and eclogite facies metamorphic rocks and briefly discuss the implications of these findings.

2 Methods

The Fe K-edge XANES method allows for in situ analysis at the micrometre-scale resolution of $Fe^{3+}/\Sigma Fe$ in minerals and glass (e.g. Wilke et al., 2001, 2004; Sutton et al., 2020; Botcharnikov et al., 2024). At the European Synchrotron Radiation Facility (ESRF), we first analysed a series of standard materials that were previously analysed by XANES and/or Mössbauer spectroscopy (Wilke et al., 2001, 2009; Schmid et al., 2003) and that represent a complete spectrum of $Fe^{3+}/\Sigma Fe$: iron, olivine, siderite, aegirine, omphacite, andradite, and glass (Table S1, Figs. S1–S2 in the Supplement). These materials included powders and larger (millimetre-scale) crystals in grain mounts. The beam from the two-pole wiggler source at BM23 was focused to $3 \times 3\,\mu m^2$ using a KB mirror, resulting in a flux of 2×10^{10} photons s^{-1} in the focal spot at 10 keV (Rosa et al., 2024). Spectra were recorded in fluorescence mode using a silicon drift detector (SDD) available from the beamline. Initially, measurements series on a single spot were performed to check for possible beam damage, which was not detected. The use of a Si (311) double-crystal monochromator together with the small source size from the newly installed Extremely Brilliant Source (EBS) and a small vertical gap of the entrance slit of the KB mirror revealed unprecedented energy resolution (0.196 eV) (Fig. 1a, b). The monochromator energy was calibrated using metallic iron, with the first maximum of the derivative at 7111.08 eV. As a result of sample preparation, Fe content, and/or sample thickness, spectra were not affected by self-absorption.

Measurements on ferric reference compounds revealed a shift of the corresponding centroid energy position (here referred to as the centroid) by +0.1 eV, which we attribute to an effect of the enhanced resolution. In order to cross-check, we have treated the newly acquired spectra and those recorded elsewhere (Fig. 1a, b) with the same procedure. In contrast, ferrous reference compounds do not show any effect (Fig. 1c). The centroid of the pre-edge is converted to an Fe oxidation state as follows:

$$Fe^{3+}/\Sigma Fe = 5915527 + 1664 \cdot \text{centroid} + 0.117 \cdot \text{centroid}^2 \text{ (error in parameters: } 1.69 \times 10^5, 47, 0.003). \quad (1)$$

This calibration applies to centro-symmetric sites, i.e. octahedral, hexahedral, and dodecahedral coordination and their distorted equivalents. The newly established calibration particularly affects samples with $Fe^{3+}/\Sigma Fe > 0.5$, as illustrated in comparison to the calibration of Wilke et al. (2009) (Fig. 1c).

Analyses were successful at all Fe contents down to 0.3 wt % FeO*. Following the analysis of reference materials, we analysed lawsonite and epidote in polished thin sections and grain mounts as follows: in each sample, typically two to four distinct crystals of lawsonite or epidote with scans on individual spots or an array of spots in a line across part or all of the crystal to evaluate Fe zoning. Two spectra were acquired for most analytical spots (see Sect. S1 in the Supplement).

3 Results

3.1 Evaluation of suitability of lawsonite and epidote crystals for XANES analysis

To evaluate the effect of crystallographic orientation on XANES spectra for orthorhombic lawsonite and zoisite and monoclinic epidote group minerals representing different compositions between epidote and clinozoisite endmembers, grain mounts were prepared from distinct orientations of large single crystals. Mineral compositions and zoning were analysed by electron microprobe at the University of Minnesota and Universität Potsdam (see Sect. S2). Crystallographic orientation was determined by electron backscattered diffraction (EBSD) at the Bayerisches Geoinstitut and the University of Minnesota (see Sect. S3).

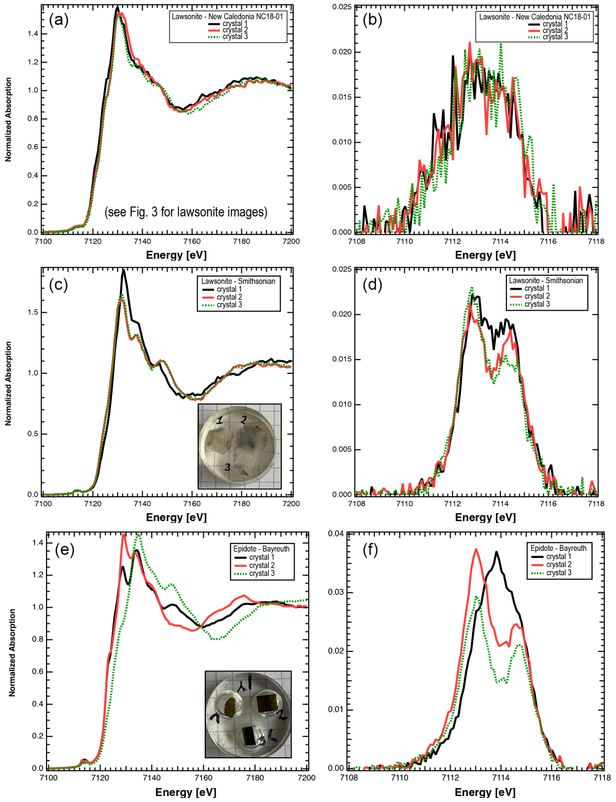

Figure 2. **(a–d)** Graphs illustrating results from lawsonite from different localities and demonstrating the relatively weak dependence on orientation. **(a)** Normalized XANES spectra of three lawsonite crystals from one blueschist, illustrating the weak variability in the spectra. **(b)** Pre-edge after background subtraction. The significant contribution at energies below 7112 eV indicates contributions by Fe^{2+}. **(c)** Normalized XANES spectra of three slices in different orientations, cut from one large crystal of lawsonite from the Franciscan Complex (Smithsonian collection), illustrating the weak dependence of spectra on orientation. **(d)** Pre-edge after background subtraction. **(e–f)** Graphs illustrating the strong dependence of epidote spectra on crystal orientation. **(e)** Normalized XANES spectra of three slices in different orientations, cut from one large crystal (Bayreuth collection). **(f)** Pre-edge after background subtraction. Analysis of the centroid leads to $Fe^{3+}/\Sigma Fe$ between 0.97–1.18. The orientation of crystal 1 {010} leads to overestimation of the true oxidation state, highlighted by the different shape of the pre-edge. The orientation of crystal 2 is close to {100}; the orientation of crystal 3 is {001}.

Grain mounts of centimetre-scale pink lawsonite crystals from two different samples from the Franciscan Complex (USA) were analysed by XANES: sample C3247 from the Smithsonian Institution's National Museum of Natural History (specific locality unknown) and a sample from the collection of the Department of Earth and Environmental Sciences, University of Minnesota (Bodega Creek locality) (Figs. 2, 3a–c). Lawsonite exhibits a very low degree of linear dichroism, i.e. virtually no orientation effect on the determined Fe oxidation state (Figs. 2, 3a–c). For comparison with results from the large single crystals, we also analysed a multi-crystal grain mount of lawsonite separated from a blueschist from Corsica from the Collections Géologiques de l'Observatoire des Sciences de l'Univers de Grenoble (OSUG 9936). In addition, during analysis of grains in thin section, we further checked for orientation effects in lawsonite by comparing spectra obtained for the same spot at different orientations; resulting centroid positions and, thus, Fe oxidation state values were essentially identical. Determined $Fe^{3+}/\Sigma Fe$ values for lawsonite are likely to be robust owing to the lack of beam damage at the applied photon dose and lack of orientation effects.

Grain mounts were also prepared from EGM single crystals that were each cut along three planes: epidote (location unknown) from the collection of the Bayerisches Geoinstitut; commercially acquired clinozoisite from a locality in Gilgit, Pakistan; and zoisite from the University of Minnesota (UMN) collection (location unknown) (Figs. 1, 2, S1). EGMs show significant variation in XANES spectra (Figs. 2, S1), and therefore the pre-edge centroid and the determined $Fe^{3+}/\Sigma Fe$ varied as a function of orientation.

3.2 Analysis of lawsonite and epidote in petrographic thin sections

We conducted XANES analysis of lawsonite and epidote/clinozoisite in thin sections of high-pressure–low-temperature (HP/LT) metabasaltic rocks: a lawsonite eclogite from Sivrihisar, Türkiye, and five samples from New Caledonia – two lawsonite blueschists, two epidote blueschists, and one epidote-bearing eclogite facies metabasite. As noted, epidote exhibits significant linear dichroism and lawsonite does not (Fig. 2), so we report quantitative data only for lawsonite.

In the Sivrihisar eclogite analysed, lawsonite contains ∼ 1.2 wt %–1.8 wt % FeO* (sample SV12-13D, Table S2; similar to SV12-13E of Fornash et al., 2019, and Fornash and Whitney, 2020). In New Caledonia blueschist NC18-01, lawsonite ranges from 0.35 wt %–1.0 wt % FeO*, with higher values typically at the rims of grains (Fig. 3, Table S2). This sample is from the low-grade end of the subduction complex. Lawsonite in blueschist sample NC19-159 contains 0.30 wt %–0.85 wt % FeO* (Table S2), with higher values at the rims of grains. This sample is from a higher-grade part of the lawsonite zone, close to the lawsonite-out–epidote-in isograd, and is inferred from petrographic observation to have had a gabbroic protolith.

A comparison of XANES measurements for lawsonite from New Caledonia samples to those from the Franciscan Complex and Corsica reveals a significant difference in the resulting $Fe^{3+}/\Sigma Fe$: an average of ∼ 0.5–0.6 compared to values of 0.9–1.05, respectively (Fig. 3). Given the documented effect of crystallographic orientation on samples free of Fe^{2+}, we can rule out any artefacts from linear dichroism.

The comparison of the pre-edge spectra shows significant contributions that can be assigned to Fe^{2+} (Fig. 2). Further, the structure of the XANES at the main edge strongly differs from that shown by all other samples, which indicates a different crystallographic site for at least parts of the incorporated iron. The broad distribution of values for New Caledonia (Fig. 3d–e) is likely related to the low Fe content, which resulted in worse counting statistics and thus in less robust background removal. Within the given error, the measured spots do not seem to show any systematic spatial variation.

4 Discussion

We report the results of XANES analyses that reveal the presence of Fe^{2+} in lawsonite in New Caledonia HP/LT rocks and in zoisite from an unknown locality (UMN collection) (Figs. 3, S1). In the following sections, we briefly discuss the possible location of Fe^{2+} in the crystal structures and the possible implications of our finding of substantial amounts of Fe^{2+} in these hydrous silicates that are important index minerals of subduction metamorphism.

4.1 Fe in lawsonite and epidote group minerals

It is not yet known what site (or sites) Fe^{2+} occupies in lawsonite and epidote group minerals. Fe^{2+} and Fe^{3+} in EGMs may occupy octahedral sites (Fehr and Heuss-Aßbichler, 1997) and/or the Ca^{2+} site, similar to the proposed sites for Fe^{2+} in lawsonite based on Mössbauer hyperfine parameters and theoretical calculations (Weber et al., 2007). Using data from a global survey of electron microprobe analyses of lawsonite from many different subduction complexes (Whitney et al., 2020; Kang et al., 2022, 2024), there appears to be no straightforward correlation of Ca and Fe, perhaps because both Fe^{2+} and Fe^{3+} are present in lawsonite.

Qualitatively, the spectra of lawsonite from the Franciscan and Corsica samples may be explained by incorporation of Fe^{3+} on the Al site. For Fe^{2+}, the Ca site is also possible, which could explain the significant difference in XANES spectra of blueschist samples from New Caledonia (Fig. 2a–b). The very strong linear dichroism observed in EGMs (e.g. Waychunas et al., 1986; this study) stems from the fact that all octahedral sites are well aligned along the *b* axis in the crystal structure (Fig. S4), which makes these minerals a unique case for studying polarized XANES spectra. In contrast, in the lawsonite structure, octahedral sites are arranged in two directions mirrored by a plane parallel to (001) (Fig. S4), so dichroism effects are less strong. Minor Fe in zoisite may exhibit behaviour similar to that in lawsonite; both are low-Fe orthorhombic minerals, in contrast to monoclinic epidote and clinozoisite.

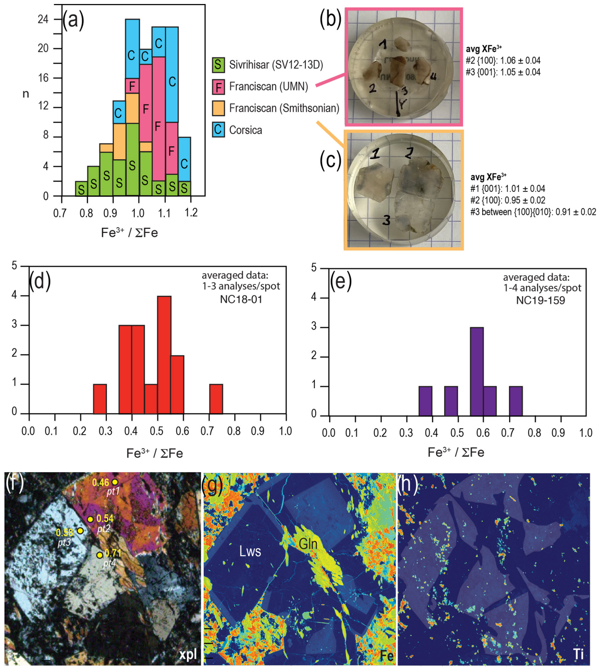

Figure 3. **(a)** $Fe^{3+}/\Sigma Fe$ calculated from XANES analysis of Fe^{3+}-rich lawsonite in eclogite (Sivrihisar, thin section) and blueschists (Franciscan Complex, slices cut at different orientations of large single crystals; Corsica, mineral separate) (Table S1). Average compositions of different slices of Franciscan lawsonite in **(b)** and **(c)** are listed with the orientation of each analysed plane (EBSD methods and data in the Supplement, Sect. S3). **(d–e)** $Fe^{3+}/\Sigma Fe$ for lawsonite in two New Caledonia blueschists. The width of the bars reflects an approximation of uncertainty, which varies with $Fe^{3+}/\Sigma Fe$ from ±0.05 for $Fe^{3+}/\Sigma Fe \leq 0.5$ to ±0.07 for > 0.5. **(f)** Photomicrograph of NC18-01 under cross-polarized light showing a cluster of lawsonite crystals, including one displaying hourglass zoning related to variation in Ti content (Table S2). Lawsonite grains are annotated with $Fe^{3+}/\Sigma Fe$ calculated from XANES. **(g–h)** Element maps obtained by electron probe microanalysis of lawsonite crystals in **(f)**, showing variation in Fe **(g)** and Ti **(h)**. Maps are highlighted by lighter shading of higher-Fe and higher-Ti regions (electron probe microanalyser (EPMA) methods and data in Sect. S2). Gln denotes glaucophane; Lws denotes lawsonite.

4.2 Implications of the presence of Fe^{2+} in lawsonite and epidote group minerals

The oxidation state of Fe in metamorphic minerals is rarely determined directly, and it is difficult to evaluate the stoichiometry of hydrous minerals that contain multi-valent cations from electron microprobe data. HP/LT rocks from various subduction complexes have previously been investigated in the context of how variation in oxygen fugacity (fO_2) influences mineral assemblages and their P–T stability in subduction zones (e.g. Brown, 1977; Mattinson et al., 2004; Poli and Schmidt, 2004; Warren and Waters, 2006). Redox conditions and effects of the oxidation state on metamorphic phase equilibria are commonly inferred using bulk-composition-specific phase diagrams (pseudosections) to evaluate the effects of varying bulk $X\mathrm{Fe}^{3+}$ on modelled mineral assemblages (e.g. López-Carmona et al., 2013; Chapman and Clarke, 2021). Typically, minerals are assumed to contain either Fe^{2+} or Fe^{3+}, and variation in $Fe^{3+}/\Sigma Fe$ is not accounted for in activity–composition relations for minerals. For example, studies that have used garnet–epidote oxybarometry to calculate fO_2 in HP/LT rocks have assumed that all Fe in epidote is Fe^{3+} and all Fe in garnet is Fe^{2+} (e.g. Gerrits et al., 2019). Preliminary results from our study suggest that epidote group minerals (with the exception of zoisite) may contain only Fe^{3+} or, to be more precise, that any potential Fe^{2+} content must be very low and cannot be resolved by XANES owing to the strong dichroism. This is consistent with previous Mössbauer data in which only epidote crystals with low Fe content yielded small contributions by Fe^{2+} (Fehr and Heuss-Aßbichler, 1997; Dollase, 1973). These studies also noted that minor contributions by impurity phases cannot be completely ruled out, as bulk measurements on powdered samples were used. Therefore, in some cases, this assumption is valid.

However, our results show that Fe^{2+} in lawsonite and zoisite in subducted oceanic crust may be greater than is currently known (Figs. 3, S1). Although these are low-Fe minerals, this finding may have implications for understanding subduction redox conditions and processes, especially across the important lawsonite–zoisite reaction during subduction and/or exhumation. The presence of substantial Fe^{2+} in some hydrous silicates and variation in $Fe^{3+}/\Sigma Fe$ within a subduction complex could be related to (1) protolith composition (e.g. extent of pre-subduction alteration of oceanic crust), and/or (2) interaction with fluids from different sources (serpentinite, sediment) that affect the oxidation state of oceanic crust during subduction. Additional XANES analyses of metabasalt across a range of metamorphic grades from different subduction complexes, as well as complementary geochemical data, are required to evaluate these possibilities.

Data availability. All data are in the Supplement or in https://doi.org/10.1016/j.chemgeo.2019.119356 (Fornash and Whitney, 2020) and https://doi.org/10.1130/GES01455.1 (Fornash et al., 2019).

Sample availability. The New Caledonia blueschist samples have International Geo Sample Numbers (IGSNs) as follows: IENHR001U for NC18-01 and IENHR005V for NC19-159.

Supplement. The supplement related to this article is available online at https://doi.org/10.5194/ejm-37-143-2025-supplement.

Author contributions. XANES data were obtained by MW, SH, AR, and DW. OM and AR optimized the beamline for microXAS measurements. FH acquired most of the EBSD data, provided an epidote sample, and assisted with plotting and interpretation of EBSD data. DW prepared the manuscript, with contributions from all co-authors. Illustrations were prepared by MW and DW.

Competing interests. The contact author has declared that none of the authors has any competing interests.

Acknowledgements. New Caledonia samples were collected with Natalia Raia. The Corsica blueschist sample was provided by Fabrice Brunet. We thank Christina Günter (U Potsdam) and Jennifer Mitchell (UMN) for support with electron microprobe analyses. We thank the ESRF for providing beamtime and the team at BM23 for technical assistance. EBSD analyses at UMN were carried out with N. Seaton in the Characterization Facility, which receives partial support from the US NSF through the MRSEC (award number DMR-2011401) and the NNCI (award number ECCS-2025124) programmes. The paper was greatly improved by reviews from Jesse Walters and the anonymous reviewer. We also thank the *EJM* editors and staff.

Financial support. This research has been supported by the National Science Foundation (grant nos. EAR-1949895 and EAR-2342604).

Review statement. This paper was edited by Giovanni De Giudici and reviewed by Jesse Walters and one anonymous referee.

References

Brown, E. H.: Phase equilibria among pumpellyite, lawsonite, epidote and associated minerals in low grade metamorphic rocks, Contrib. Mineral. Petrol., 64, 123–136, 1977.

Botcharnikov, R., Wilke, M., Garrevoet, J., Portnyagin, M., Klimm, K., Buhre, S., Krasheninnikov, S., Almeev, R., Moune, S., and Falkenberg, G.: Confocal μ-XANES as a tool to analyze Fe oxidation state in heterogeneous samples: the case of melt inclusions in olivine from the Hekla volcano, Eur. J. Mineral., 36, 195–208, https://doi.org/10.5194/ejm-36-195-2024, 2024.

Chantel, J., Mookherjee, M., and Frost, D. J.: The elasticity of lawsonite at high pressure and the origin of low velocity layers in subduction zones, Earth Planet. Sci. Lett., 349–350, 116–125, https://doi.org/10.1016/j.epsl.2012.06.034, 2012.

Chapman, T. and Clarke, G. L.: Cryptic evidence for the former presence of lawsonite in blueschist and eclogite, J. Metamorph. Geol., 39, 343–362, https://doi.org/10.1111/jmg.12578, 2021.

Dollase, W. A.: Mössbauer spectra and iron distribution in the epidote group minerals, Zeitschr. Kristall., 138, 41–63, 1973.

Fehr, K. T. and Heuss-Aßbichler, S.: Intracrystalline equilibria and immiscibility along the join clinozoisite–epidote: An experimental and ^{57}Fe Mössbauer study, Neues Jb Miner. Ab., 172, 43–76, 1997.

Fornash, K. F. and Whitney, D. L.: Lawsonite-rich veins and layers as archives of fluid and element cycling at the slab-mantle interface (Sivrihisar Massif, Turkey), Chem. Geol., 533, 119356, https://doi.org/10.1016/j.chemgeo.2019.119356, 2020.

Fornash, K. F., Whitney, D. L., and Seaton, N. C. A.: Lawsonite composition and zoning as an archive of metamorphic processes in subduction zones, Geosphere, 15, 24–46, https://doi.org/10.1130/GES01455.1, 2019.

Frei, D., Liebscher, A., Franz, G., and Dulski, P.: Trace element geochemistry of epidote minerals, Rev. Mineral. Geochem., 56, 553–605, 2004.

Gerrits, A. R., Inglis, E. C., Dragovic, B., Starr, P. G., Baxter, E. F., and Burton, K. W.: Release of oxidizing fluids in subduction zones recorded by iron isotope zonation in garnet, Nat. Geosci., 12, 1029, https://doi.org/10.1038/s41561-019-0471-y, 2019.

Grodzicki, M., Heuss-Assbichler, S., and Amthauer, G.: Mössbauer investigations and molecular orbital calculations, Phys. Chem. Minerals., 28, 675–681, 2001.

Hernández-Uribe, D. and Tsujimori, T.: Progressive lawsonite eclogitization of the oceanic crust: Implications for deep mass transfer in subduction zones, Geology, 51, 678–682, https://doi.org/10.1130/G51052.1, 2023.

Kang, P., Whitney, D. L., Martin, L. A. J., and Fornash, K. F.: Lawsonite trace-element record of subduction fluids, J. Petrol., 63, 1–32, https://doi.org/10.1093/petrology/egac065, 2022.

Kang, P., Martin, L. A. J., Vitale Brovarone, A., and Whitney, D. L.: Lawsonite and garnet oxygen isotope record of fluid-rock interaction during subduction, Geochem. Geophys., 25, e2023GC011389, https://doi.org/10.1029/2023GC011389, 2024.

Kita, S., Okada, T., Nakajima, J., Matsuzawa, T., and Hasegawa, A.: Existence of a seismic belt in the upper plane of the double seismic zone extending in the along-arc direction at depths of 70–100 km beneath NE Japan, Geophys. Res. Lett., 33, L24310, https://doi.org/10.1029/2006GL028239, 2006.

López-Carmona, A., Pitra, P., and Abati, J.: Blueschist-facies metapelites from the Malpica-Tui Unit (NW Iberian Massif): phase equilibria modelling and H_2O and Fe_2O_3 influence in high-pressure assemblages, J. Metamorph. Geol., 31, 263–280, https://doi.org/10.1111/jmg.12018, 2013.

Martin, L. A. J., Rubatto, D., Vitale Brovarone, A., and Hermann, J.: Lawsonite eclogite facies metasomatism of a granulite sliver associated to ophiolites in Alpine Corsica, Lithos, 125, 620–640, 2011.

Martin, L. A. J., Hermann, J., Gauthiez-Putallaz, L., Whitney, D. L., Fornash, K. F., and Evans, N.: Lawsonite geochemistry and stability – Implications for trace element and water cycles in subduction zones, J. Metamorph. Geol., 32, 455–478, https://doi.org/10.1111/jmg.12093, 2014.

Mattinson, C. G., Zhang, R. Y., Tsujimori, T., and Liou, J. G.: Epidote-rich talc-kyanite-phengite eclogites, Sulu terrane, eastern China: P-T-fO_2 estimates and the significance of the epidote-talc assemblage in eclogite, Am. Mineral., 89, 1772–1783, 2004.

Muñoz-Montecinos, J., Angiboust, S., Garcia-Casco, A., Glodny, J., and Bebout, G.: Episodic hydrofracturing and large-scale flushing along deep subduction interfaces: Implications for fluid transfer and carbon recycling (Zagros Orogen, southeastern Iran), Chem. Geol., 571, 120173, https://doi.org/10.1016/j.chemgeo.2021.120173, 2021.

Poli, S. and Schmidt, M. W.: Experimental subsolidus studies on epidote minerals, Rev. Mineral. Geochem, 56, 171–195, 2004.

Rosa, A. D., Garbarino, G., Rodrigues, J. E., Mijit, E., Jacobs, J., Bugnazet, D., Pasternak, S., Berruyer, G., Moyne, A., Clavel, C., Perrin, F., Anzellini, S., Meneghini, C., Occelli, F., Zhan, X., Ishimatsu, N., Sakai, T., Boccato, S., Torchio, R., Hernandez, J.-A., Heat, C. J. S., Dominijanni, S., Morard, G., Antonangeli, D., Petitdemange, S., Wehinger, B., Mezouar, M., Kovalskii, G., Morgenroth, W., Wilke, M., Di Cicco, A., Bouhifd, M. A., Irifune, T., Lomachenko, K. A., and Mathon, O.: New opportunities for high pressure X-ray absorption spectroscopy at ID24-DCM and BM23 with the Extremely Brilliant Source of the ESRF, High Pressure Research, 1–29 pp., https://doi.org/10.1080/08957959.2024.2364281, 2024.

Schmid, R., Wilke, M., Oberhänsli, R., Janssens, K., Falkenberg, G., Franz, L., and Gaab, A.: Micro-XANES Determination of ferric iron and its application in thermobarometry, Lithos, 70, 381–392, 2003.

Schmidt, M. W. and Poli, S.: The stability of lawsonite and zoisite at high pressures: experiments in CASH to 92 kbar and implications for the presence of hydrous phases in subducted lithosphere, Earth Planet. Sci. Lett., 124, 105–118, 1994.

Shiraishi, R., Muto, J., Tsunoda, A., Sawa, S., and Suzuki, A: Localized deformation of lawsonite during cold subduction, J. Geophys. Res.-Solid Earth, 127, e2021JB022134, https://doi.org/10.1029/2021JB022134, 2022.

Spandler, C., Hermann, J., Arculus, R., and Mavrogenes, J.: Redistribution of trace elements during prograde metamorphism from lawsonite blueschist to eclogite facies: Implications for deep subduction-zone processes, Contrib. Mineral. Petrol., 146, 205–222, https://doi.org/10.1007/s00410-003-0495-5, 2003.

Sutton, S. R., Lanzirotti, A., Newville, M., Dyar, M. D., and Delaney, J.: Oxybarometry and valence quantification based on microscale X-ray absorption fine structure (XAFS) spectroscopy of multivalent elements, Chem. Geol., 531, 119305, https://doi.org/10.1016/j.chemgeo.2019.119305, 2020.

Vitale Brovarone, A., Alard, O., Beyssac, O., Martin, L., and Picatto, M.: Lawsonite metasomatism and trace element recycling in subduction zones, J. Metamorph. Geol., 32, 489–514, https://doi.org/10.1111/jmg.12074, 2014.

Warren, C. J. and Waters, D. J: Oxidized eclogites and garnet-blueschists from Oman: P-T path modelling in the NCFMASHO system, J. Metamorph. Geol., 24, 783–802, https://doi.org/10.1111/j.1525-1314.2006.00668.x, 2006.

Waychunas, G. A., Brown, G. E, and Apted, M. J.: X-ray K-edge absorption spectra of Fe minerals and model compounds: II. EXAFS, Phys. Chem. Minerals, 13, 31–47, 1986.

Weber, S.-U., Grodzicki, M., Geiger, C. A., Lottermoser, W., Tippelt, G., Redhammer, G. J., Bernroider, M., and Amthauer, G.:

^{57}Fe Mössbauer measurements and electronic structure calculations on natural lawsonites, Phys. Chem. Mineral., 34, 1–9, https://doi.org/10.1007/s00269-006-0121-y, 2007.

Whitney, D. L., Fornash, K. F., Kang, P., Ghent, E. D., Martin, L., Okay, A. I., and Vitale Brovarone, A.: Lawsonite composition and zoning as tracers of subduction processes: a global review, Lithos, 370–371, 105636, https://doi.org/10.1016/j.lithos.2020.105636, 2020.

Wilke, M., Farges, F., Petit, P. E., Brown, G. E., and Martin, F.: Oxidation state and coordination of Fe in minerals: an Fe K XANES spectroscopic study, Am. Mineral., 86, 714–730, 2001.

Wilke, M., Hahn, O., Woodland, A. B., and Rickers, K.: The oxidation state of iron determined by Fe K-edge XANES – application to iron gall ink in historical manuscripts, J. Anal. At. Spectrom., 24, 1364–1372, https://doi.org/10.1039/b904438h, 2009.

Wilke, M., Partzsch, G. M., Bernhardt, R., and Lattard, D.: Determination of the iron oxidation state in basaltic glasses using XANES at the K-edge, Chem. Geol., 213, 71–87, https://doi.org/10.1016/j.chemgeo.2004.08.034, 2004.